PAPER

# Experimental studies of ion flow near the sheath edge in multiple ion species plasma including argon, xenon and neon



IOP Publishing Plasma Sources Science and Technology
Plasma Sources Sci. Technol. **26** (2017) 055021 (7pp) https://doi.org/10.1088/1361-6595/aa6776

# Experimental studies of ion flow near the sheath edge in multiple ion species plasma including argon, xenon and neon

**Greg Severn[1], Chi-Shung Yip[2], Noah Hershkowitz[2] and Scott D Baalrud[3]**

[1] Department of Physics & Biophysics, University of San Diego, San Diego, CA 92110, United States of America
[2] Department of Engineering Physics, University of Wisconsin, Madison, WI 53706, United States of America
[3] Department of Physics and Astronomy, University of Iowa, Iowa City, IA 52242, United States of America

E-mail: severn@sandiego.edu

Received 30 December 2016, revised 7 March 2017
Accepted for publication 17 March 2017
Published 11 April 2017


**Abstract**

The Bohm sheath criterion was studied with laser-induced fluorescence (LIF) in three ion species plasmas using two tunable diode lasers. It was found in the first LIF studies of three ion species plasma (Yip *et al* 2016 *Phys. Plasmas* **23** 050703) in which krypton was added to a mixture of argon and xenon plasma confined in a multidipole, dc hot filament discharge, that the addition of krypton served to turn off instability enhanced collisional friction (IEF) found in two ion species plasma (Yip *et al* 2010 *Phys. Plasmas*). In this study, neon, a less massive atomic gas than argon was added. Argon and xenon ion velocity distribution functions (IVDFs) were measured at the sheath-presheath boundary near a negatively biased boundary plate, and the $Ne^+$ density was systematically increased. We found in both cases that once the added ion density significantly exceeded the density of the other two ions, IVDF measurements consistent with the absence of the instability were obtained, and the measured ion sheath edge speeds tended toward their individual Bohm velocities. For all other relative concentrations, the ions reached the sheath edge neither at their Bohm speeds nor the ion sound speed of the system, consistent, qualitatively, with the action of the IEF.

Keywords: sheath formation, Bohm's criterion, multiple ion species plasma, laser-induced fluorescence, kinetic theory

## 1. Introduction

Plasma sheaths [1, 2] are non-neutral regions that form at plasma boundaries to balance electron and ion losses. They are the most ubiquitous feature of bounded plasma. The Bohm criterion [2, 3] in a single ion species plasma asserts that positive ions equal or exceed the sound speed at the sheath boundary in order for a stable sheath to form at the material bounding the plasma. This notion underpins discussions throughout plasma physics [4], including probe diagnositics [5], plasma processing [6], astrophysical plasmas [4], and even plasma-wall interactions in the context of fusion research [7, 8]. Since the terms sheath and plasma arose at the same time in pioneering studies in the early 1920s, nearly 100 years ago, it is often assumed that the assumptions underlying theories of sheath formation have been richly benchmarked by direct experiment. This is beginning to be true for one and two ion species weakly collisional, electropositive plasmas, where a comparison to the Bohm Criterion generalized to multiple ion species has now been done for two-ion species plasmas [9]. It is important to note that the test of Bohm's criterion in two ion species plasmas revealed unexpected results [10, 11] which were treated by a novel application of the kinetic theory of streaming instabilities developed by Baalrud, Callen, and Hegna [12, 13] in the presheath-sheath boundary region, the theory of instability enhanced collisional

 

friction (IEF), and which were validated to a significant extent [14–16]. Measured instabilities associated with the IEF were presented previously [11, 14]. In addition, PIC simulation has predicted both the existence of these instabilities and a causal relation between these instabilities and the frictional force [17].

Simple experimental tests of Bohm's criterion are still lacking at higher pressure cases where the ion-neutral mean free path is comparable with the Debye length. In this regime (and only for single ion species plasmas) there are a great many theoretical works, [18–23] but no experiments confirm which of the manifestly different theoretical results are correct. It is fair to say that all agree that for single species plasmas the ions will be subsonic at the sheath edge. Our paper does not address this problem. It is also true that benchmarking experiments are are still lacking in the case of electronegative plasmas, and our work does not address this problem either.

Our paper addresses the problem of sheath formation in three ion species, weakly collisional, electropositive plasmas in which the IEF instability mechanism was expected to affect ion flow at the end of the presheath near the plasma boundary. We extend the results of our very recent work with argon–krypton–xenon plasmas in which we demonstrated [24] that the IEF led to the result that under most circumstances, the ions do not reach the sheath edge at either their individual Bohm speeds or the ion sound speed of the system. In that work the conditions for which IEF become unstable were observed to be altered with the addition of an ion species of intermediate mass, namely krypton. In the present work we show that when an ion of smaller mass than either xenon or argon is added, the phenomena is more complex, and yet the IEF remains the determining factor controlling sheath edge flow speeds until that light ion density dominates.

In section 2 we describe the experiment and diagnostics, in section 3, the physics of the model we use to estimate the ion concentrations. In section 4, we present a theoretical model of the IEF in three ion species plasmas, and in section 5 we discuss our results and conclusions.

## 2. Experimental details

Plasma was produced in a multidipole chamber through impact ionizations of energetic primary electrons emitted by hot thoriated tungsten filaments biased at −60V with respect to the grounded chamber wall. The base pressure of the chamber was approximately 0.5 $\mu$Torr. 0.1 mTorr argon and 0.04 mTorr xenon were added to the chamber to create an approximately 55–45 mix of Ar–Xe ion plasma. Krypton (0–0.14 mTorr) or neon (0–5 mTorr) was then added to create three ion species plasmas, with a neutral pressure that is the sum of all three constituents. A Langmuir probe with a 6.4 mm diameter double sided disc was inserted from the end wall opposite to the one which tungsten filaments were installed to measure the plasma density $n_e$ and the electron temperature $T_e$. An emissive probe was inserted from the same end wall as the Langmuir probe to measure the plasma

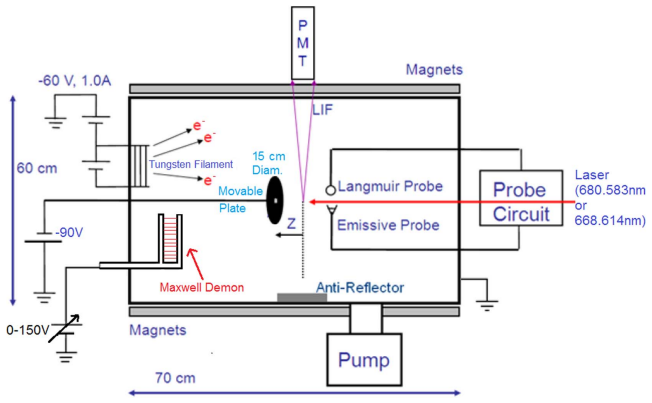


**Figure 1.** A schematic diagram of the experimental setup.

potential $V_p$ using the inflection point technique in the limit of zero emission. A MacKenzie's Maxwell Demon [25, 26] was employed to control $T_e$ at 1.95 ± eV. The system sound speed $c_s$ was determined by measuring the ion acoustic wave (IAW) phase velocity of a continuous wave launched from a 10 cm diameter grid with the direct coupling filtered by a boxcar averager [27]. A movable 15 cm diameter plate on axis of the chamber was biased at −90 V to create a sheath-presheath structure. A schematic of the multidiople chamber is shown in figure 1.

Ion velocity distribution functions (IVDFs) of $Ar^+$ and $Xe^+$ ions were directly, non-invasively measured through the employment of laser induced fluorescence (LIF). Two tunable diode lasers were employed to separately measure ArII and XeII metastable ions in the system. XeII LIF was obtained by exciting ions in the metastable state $5p^4\,(^3P_1)5d\,[3]_{7/2}$ to the $5p^4\,(^3P_1)6p\,[2]^0_{5/2}$ excited state with a laser wavelength centered at 680.580 nm (in air) finely tuned over a 10 GHz range. The excited ions spontaneously emit at 492.15 nm wavelength (in air) and decay to the $5p^4\,(^3P_1)6s\,[1]_{3/2}$. ArII LIF was obtained through exciting metastables in the $4s^4P_{3/2}$ state to the $4p^4D^0_{5/2}$ at 668.614 nm (vacuum). Spontaneous emission is measured at 442.6 nm (vacuum) in the decay to the $4s^4P_{3/2}$ state. The collection optics consist of an objective lens, an iris at the focal plane of the diagnosed volume, a short focal length lens placed one focal length from the iris so that light collected from the diagnosed is normally incident upon the interference filters, and then upon a face-on photomultiplier tube, as shown in figure 1. The movable biased plate was moved so as to cause the sheath-presheath structure to pass through the diagnosed volume (fixed by the location of the collection optics) to permit measurement of axial profiles of the LIF. The LIF signal was collected as a function of detuning frequency, $\Delta\omega$, and a change of variables was performed using the first order Doppler shift equation, $\Delta\omega = k_l v_z$. This gives the LIF signal as a function of velocity (the component of the velocity along the beam, and normal to the movable boundary plate) and while not the equivalent of the IVDF, it is proportional to it. This constant of proportionality cancels out in the velocity space averaged calculations of the flow speeds.

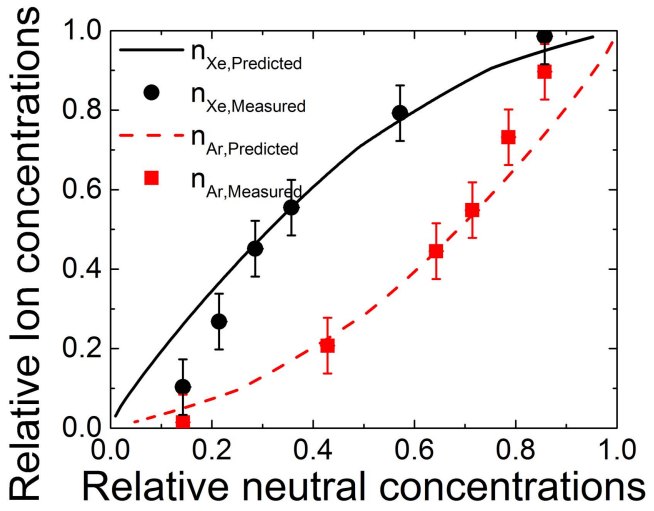


**Figure 2.** Measured Xe–Ar relative ion concentrations compared with predictions using the modified model of [28].

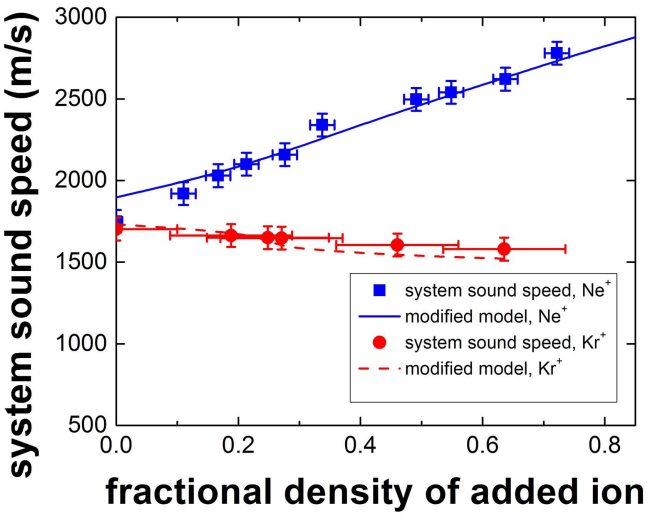


**Figure 3.** Measured ion sound speeds compared with the calculated ion sounds speed graphed against the fractional densities of the added ion using results of the modified version of the model of Kim *et al* 0–0.14 mTorr krypton and 0–5 mTorr neon gases were added to 0.14 mTorr argon–xenon plasmas.

## 3. Estimation of ion densities

Recent work by Kim *et al* [28] developed a model to estimate the relative ion concentrations in two-ion species plasmas created in a multi-dipole confined filament discharge. Through balancing the relative ion production predominately by primary electron impact and the relative ion loss predominately to the walls, Kim *et al* showed that

$$\frac{n_1}{n_2} = \frac{n_{n,1} n_{\mathrm{pri}} \sigma_1(E_{\mathrm{PE}})}{v_1 A_{\mathrm{Wall}}} \frac{v_2 A_{\mathrm{Wall}}}{n_{n,2} n_{\mathrm{pri}} \sigma_2(E_{\mathrm{PE}})}, \quad (1)$$

where $n_1$ and $n_2$ are the ion densities, $n_{n,1}$ and $n_{n,2}$ are the neutral densities, $n_{\mathrm{pri}}$ is the primary electron density, $A_{\mathrm{Wall}}$ is the ion loss area to the chamber wall, $\sigma_1$ and $\sigma_2$ are the electron impact ionization cross sections at the primary electron energy $E_{\mathrm{PE}}$, and where $v_1$ and $v_2$ are the respective loss velocities at the sheath-edge of the two ion species respectively. The ion loss velocities for two-ion species plasmas was calculated from the IEF theory determining the generalized Bohm criterion for two ion species. Such calculation requires solving a system of equations including equation (1), the generalized Bohm criterion, the IEF condition (described below) and the condition of quasi-neutrality, $n_1 + n_2 = n_e$.

To demonstrate that this model was suitable for use in our particular plasma source, we employed it to predict the relative ion concentrations of our previous experiments. Figure 2 shows relative ion concentration data [29] in Xe–Ar plasmas measured in our multi-dipole filament discharge compared with predictions using the production-loss balance equation. It is clear that good agreement between the previous experimental result and the theoretical predictions is achieved.

To extend the model to the three ion species plasmas in our system, we similarly compared the loss-production rates between the different ion species. Specifically, we applied equation (1) with argon being species 1 and xenon or the third ion species being species 2. The resultant ratios (e.g., $n_2/n_{\mathrm{Ar}}$) were then normalized by $(1 + n_{\mathrm{Xe}}/n_{\mathrm{Ar}} + n_3/n_{\mathrm{Ar}})$ to obtain the relative ion concentration of each species. In addition, we applied the LIF measured ion drift velocities at the sheath/presheath boundary to obtain the argon and xenon ion loss velocities required in equation (1). The resolution of the ion loss velocities of the third ion species is described as follows.

To obtain a reasonable estimation of relative ion densities of Ne–Ar–Xe plasmas, we resolved the self-consistent equations for the neon (krypton) ion drift velocity and the relative densities in the following loop: resolved Kim *et al*'s production-loss balance equations mentioned above using the measured neutral pressures of the three ion species, the measured primary energy and the measured xenon and argon escape velocities. Starting with these measured parameters, we first assumed that the neon (krypton) ions were lost at their individual Bohm velocities and obtained an approximation of the relative ion densities with Kim *et al*'s equations mentioned above. We then used this approximate relative ion concentration to calculate the neon (krypton) ion sheath edge velocity using the generalized Bohm criterion. Then the new neon sheath edge velocity was used again to estimate the relative ion densities. The loop of calculating the escape velocity and relative ion concentration was repeated until convergence was reached.

Figure 3 shows the resultant ion sound speed of the system calculated from the model in this manner, along with the actual ion acoustic speed measured in the bulk plasma. The figure is no more than a gross check of the consistency of the model and experimental results despite the fact that the model curves agree with the measurements within experimental error. Where krypton is added to a plasma comprising roughly equal concentrations of argon and xenon, the ion sound speed of the system is expected to fall as a result of the increased average ion mass, though weakly, as its mass is intermediate between that of argon and xenon, and of course

the opposite is expected where neon is added under the same initial conditions. But the experimental uncertainty in these IAW measurements, particularly obvious in the krypton data set, is large enough to admit a perfectly flat trend that is independent of the addition of krypton. Further both data sets are graphed versus the model estimates of the relative concentration of the added ion, whether neon or krypton, which assumes that the argon and xenon ion concentrations remained unchanged, thus, the comparison graphed in figure 3 is not a direct experimental test of that particular assumption. Nevertheless, it is clear that that assumption is not obviously a bad one.

## 4. Theoretical model

Assuming Maxwellian distributions, and looking for waves satisfying $\omega \ll kv_{Te}$, the electrostatic dielectric function in a plasma with 3 species of ions is

$$\hat{\varepsilon} = 1 + \frac{1}{k^2\lambda_{\mathrm{De}}^2}\sum_{i=1}^{3}\left[1 - \frac{z_i^2}{2}\frac{T_e}{T_i}\frac{n_i}{n_e}Z'\left(\frac{\omega - k\cdot v_i}{kv_{T_i}}\right)\right], \quad (2)$$

where $Z$ is the plasma dispersion function, and the prime denotes its first derivative with respect to the argument. Here $v_{Ti} = \sqrt{2T_i/m_i}$ for each ion species $i = 1, 2, 3$, $k$ is the wavenumber and $z_i$ are the ion charges. In the solutions that follow, stability boundaries and sheath edge flow speeds are obtained from solving $\hat{\varepsilon} = 0$ numerically directly from equation (2). We attempt to answer the question: how does the speed that each ion species attains at the sheath edge change if one starts with a mixture with equal concentrations of $Ar^+$ and $Xe^+$, then adds $Kr^+$ or $Ne^+$? Furthermore, how much of the third species must be added to entirely turn off the two-stream instability throughout the presheath? The IEF would be effectively turned off for cases in which argon and xenon ions reach the sheath edge at their individual Bohm speeds.

The following discussion follows closely the model introduced in our previous work [24] that treated the case in which the third ion species added was intermediate in mass between Ar and Xe, namely Kr. Here we introduce a modification of that model which makes the model less dependent on assumptions as yet unsubstantiated by experiment, and we use it to treat the case in which the third ion species is less massive than the other two, namely Ne. Here we use the labels: 1 = Ar, 2 = Kr and 3 = Xe (lightest to heaviest) to denote the different species, for the case that Kr II is the added ion. Here, $z_1 = z_2 = z_3 = 1$, and we assume that all ion temperatures are the same, $T_1 = T_2 = T_3 = T_i$. We assume, in agreement with the experimental results, that argon and xenon concentrations are approximately equal, so:

$$\frac{n_1}{n_e} = \frac{n_3}{n_e} = \frac{1}{2}\left(1 - \frac{n_2}{n_e}\right). \quad (3)$$

We consider different values of $n_2/n_e$.

The critical differential flows at which the two-stream instability arises are calculated from equation (2) in the following way. First, it is useful to redefine the arguments of the plasma dispersion functions, which we note are dimensionless: $\xi_i = (\omega - k\cdot v_i)/kv_{Ti}$. We introduce the auxiliary variable $\Omega$ via the relation

$$\omega = \frac{1}{2}k\cdot(v_1 + v_3) + k\cdot\Delta v_{13}\Omega. \quad (4)$$

Then, $\omega - k\cdot v_1 = k\cdot\Delta v_{13}(\Omega - 1/2)$, $\omega - k\cdot v_2 = k\cdot\Delta v_{12} + k\cdot\Delta v_{13}(\Omega - 1/2)$, and $\omega - k\cdot v_3 = k\cdot\Delta v_{13}(\Omega + 1/2)$, where $\Delta v_{13} = v_1 - v_3$ and $\Delta v_{12} = v_1 - v_2$. This is useful because now the arguments of the plasma dispersion function ($\xi_i = (\omega - k\cdot v_i)/kv_{Ti}$) in equation (2) can be written in terms of the differential flow speed between species 1 and 2 and the differential flow speed between species 1 and 3:

$$\xi_1 = \Delta\bar{v}_{13}(\Omega - 1/2), \quad (5a)$$

$$\xi_2 = \sqrt{\frac{T_1}{T_2}\frac{m_2}{m_1}}(\Delta\bar{v}_{12} + \Delta\bar{v}_{13}(\Omega - 1/2)), \quad (5b)$$

$$\xi_3 = \sqrt{\frac{T_1}{T_2}\frac{m_3}{m_1}}\Delta\bar{v}_{13}(\Omega + 1/2), \quad (5c)$$

where the $\Delta\bar{v}_{13} = \Delta v_{13}/v_{T1}$, where the bar denotes speed in units of $v_{T1}$. Finally, taking the limit of small $k$, and assuming that all ion species have the same temperatures, then equation (2) allows us to find the zeroes of the function $f(V_c)$ to solve for the threshold condition for the critical differential flows:

$$f(\Delta V_c) \approx z_1^2 x_1 Z'(\xi_1) + z_2^2 x_2 Z'(\xi_2) + z_3^2 x_3 Z'(\xi_3) - 2T_i/T_e = 0, \quad (6)$$

subject of course to the quasineutrality constraint: $z_1x_1 + z_2x_2 + z_3x_3 = 1$. Here, $x_1 = n_1/n$ is the concentration of species 1, and $z_1$ refers to the ion charge (which we assume to be 1 here).

Equation (6) is solved for the threshold speed between species 1 and 3 ($\Delta v_{13}$) assuming $\Delta v_{12}$ is known from another constraint (discussed below). The system of equations is then closed using the generalized Bohm criterion, which in the units above can be written:

$$x_1\frac{1}{(\Delta\bar{v}_{12} + \bar{v}_2)^2} + x_2\frac{m_1}{m_2}\frac{1}{\bar{v}_2^2} + x_3\frac{m_1}{m_3}\frac{1}{(\Delta\bar{v}_{12} + \bar{v}_2 - \Delta\bar{v}_{13})^2} = 2\frac{T_1}{T_e}. \quad (7)$$

In our previous work, the additional constraint to provide $\Delta v_{12}$ was obtained by assuming that the speed of the intermediate mass species ($v_2$, which was Kr in that case) was its own sound speed at the sheath edge. Here, we would like arrive at a model independent of that assumption since we cannot yet measure the ion flows for the third ion. To do so, consider the evolution of the differential flow speeds from the bulk through the presheath. In the absence of any collisions (including ion-neutral or ion–ion), we would expect ballistic motion of the ions in response to the potential drop through the presheath. Energy conservation would then give $v_i = \sqrt{2e\Delta\phi/m_i}$ for each species $i$. Plugging this into the

Bohm criterion provides $e\Delta\phi = T_e/2$, so $v_i = c_{si}$. This is the traditional solution. It has been shown (see for example Meige *et al* [30]) that if one considers modest energy loss due to the ion-neutral friction, a larger presheath potential drop arises, but the ion flow speeds at the sheath edge remain the same. This implies that to a first approximation, ion-neutral drag does not significantly influence the differential ion flow speed. The only time one gets something different is if one ion species has a much larger neutral drag than the other, and this is not considered in the model described here.

We assume then that ion-neutral drag does not influence the difference in ion flow speeds: $\Delta v_{ij}$. We use ballistic motion to relate the difference in ion flow speeds from the bulk plasma, through the presheath, up to the point that instability-enhanced friction acts (if that occurs somewhere along the presheath). Ballistic motion implies

$$\Delta\bar{v}_{12} = \sqrt{\frac{e\Delta\phi}{T_i}}\left(1 - \sqrt{\frac{m_1}{m_2}}\right), \quad \text{and}$$
$$\Delta\bar{v}_{13} = \sqrt{\frac{e\Delta\phi}{T_i}}\left(1 - \sqrt{\frac{m_1}{m_3}}\right). \tag{8}$$

The bar symbol denotes $\Delta\bar{v}_{ij} = \Delta v_{ij}/v_{T1}$. This provides a relation between $\Delta\bar{v}_{12}$ and $\Delta\bar{v}_{13}$

$$\Delta\bar{v}_{12} = \Delta\bar{v}_{13}\frac{1 - \sqrt{m_1/m_2}}{1 - \sqrt{m_1/m_3}}. \tag{9}$$

Now, ignoring ion-neutral collisions, the ions flow through the presheath essentially ballistically (satisfying equation (9)) until they run into the instability threshold condition. After that point, we will assume that the flow differences between each species ($\Delta v_{ij}$) is locked to the value at which instability first onset (i.e., the threshold condition). Since all differential flows get locked at this point of onset, a central assumption in this model, the relationship from equation (9) will also be satisfied in the region with instability. In other words, equation (9) is valid in both the instability-free region of the presheath (because of ballistic flow), and in the unstable region (because of locked differential flows). Thus, equation (9) provides the closure we are after.

The computation was carried out as follows. Figure 4 shows a plane of $\Delta\bar{v}_{12}$ versus $\Delta\bar{v}_{13}$, along with the line defined by equation (9) (black line). The dashed lines denote $\Delta v_{12} = c_{s1} - c_{s2}$ and $\Delta v_{13} = c_{s1} - c_{s3}$, which are the maximum possible values of these flow differences in the presheath. As the species enter the presheath, the flow differences begin at a low value (bottom left corner). As they fall through the presheath, these increase along the solid line shown in the figure (following the arrow), which is defined by equation (9). They proceed along this line until they run into the instability threshold (either mode 1 or mode 2, which ever has the lower threshold). After this point, the flow differences are locked to these values. If the thresholds for instability are above the dashed lines, then there is no instability in the presheath, and we say that each species has it is own sound speed at the sheath edge. Note that in figure 4, we chose $T_e/T_i = 1.95/0.026 = 75$, $x_1 = 0.3$, and assumed $x_2 = x_3$ (the species are Ne, Ar and Xe) for the illustration. Finally, we put the $\Delta v$ values from figure 4 into the Bohm criterion and solved for each of the individual flow speeds. The result is shown in figures 5 and 6.

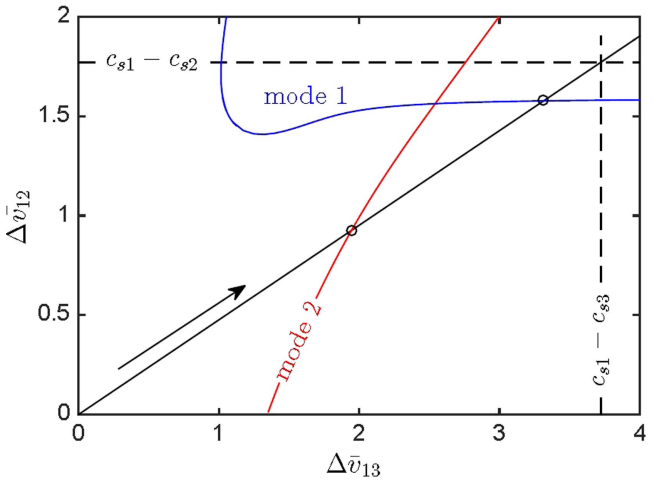


**Figure 4.** Illustration of the evolution of flow differences through the presheath for $T_e/T_i = 1.95/0.026 = 75$, $x_1 = 0.3$, and assumed $x_2 = x_3$ (the species are Ne, Ar and Xe). There are two possible unstable modes here, we only need to identify the one with the lowest threshold for instability (along the solid line). In this case, it is mode 2.

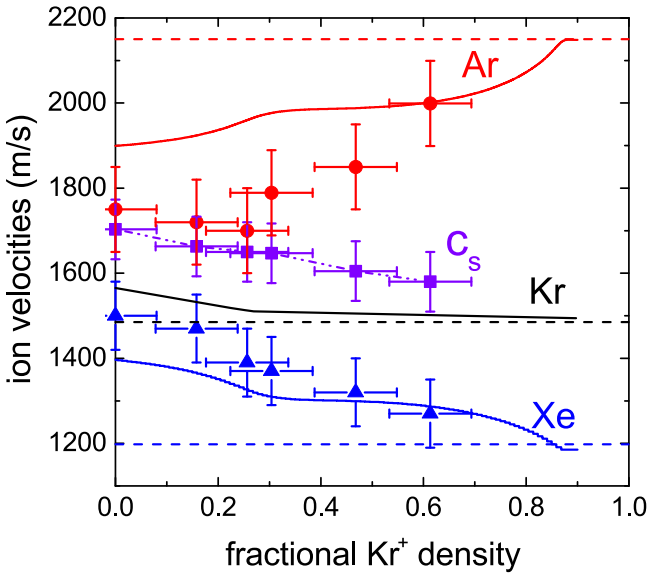


**Figure 5.** Velocities at the sheath edge for argon (red) and xenon (blue online). The theory calculations assumed $T_e/T_i = 1.95/0.026 = 75$, and assumed $x_1 = x_3$. Theory curves are solid lines, given for all three ions, krypton in black, and the individual sounds speeds are indicated by dashed lines. For all data points in this figure $T_e = 1.95 \pm 0.08$ eV.

## 5. Results and discussion

At the outset of the discussion of the theoretical model in section 4, we noted that a clear indication of the streaming instability turning off was that the ion flow speeds became

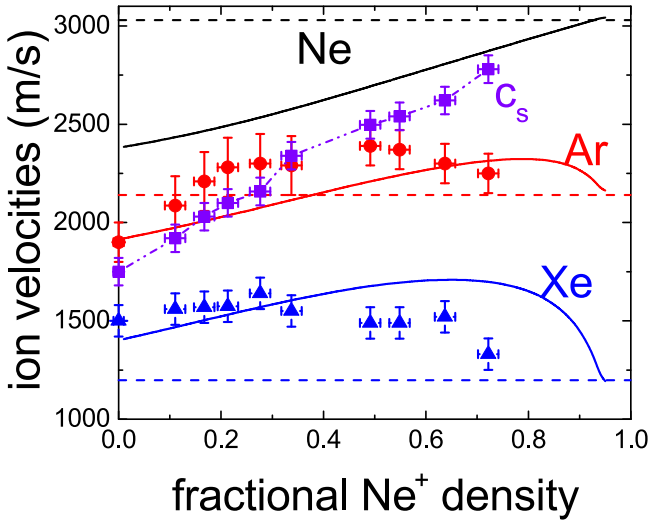


**Figure 6.** Velocities at the sheath edge argon (red), and xenon (blue online). The theory calculations assumed $T_e/T_i = 1.95/0.026 = 75$, and assumed $x_2 = x_3$. Theory curves are solid lines, given for all three ions, neon in black, and the individual sound speeds are indicated by dashed lines. For all data points in this figure $T_e = 1.95 \pm 0.08$ eV.

their individual Bohm speeds at the sheath edge, whether measured or calculated. Also, a central practical concern was about the amount of a third ion density needed to turn off the instability. Heuristically, one could assume that the effect of adding neon to a streaming unstable two ion plasma in the presheath region is different than that of adding krypton. For an ion population already unstable with two separated warm peaks in velocity space with the critical $\Delta v$ between argon and xenon calculated in section 4, the addition of a third ion component with an intermediate mass would serve to fill up the valley in velocity space between the argon and xenon peaks, whereas the addition of neon, less massive than both, is expected to add a third peak and a second valley, and therefore not cause to increase the velocity space gap between argon and xenon peaks at which the IEF turns on, at least not for small and intermediate fractional densities. We argue here that data and theory support this qualitative argument.

In figure 5 we see evidence that the addition of krypton increases the critical $\Delta v_{13}$ (argon, 1, xenon, 3, numbered in order of increasing mass) as the relative concentration of krypton grows. The solid lines are model calculations indicating the flow speeds in the presheath at which the system becomes marginally unstable because the IEF turns on. This occurs some spatial distance before the end of the presheath as the ions pick up speed on the way to the sheath edge. The instability then locks the velocity difference the rest of the way to the sheath, and so yields an estimate of the sheath edge flow speeds. That $\Delta v_{13}$ increases with the relative krypton density indicates that the former critical velocity difference between argon and xenon ions is no longer unstable even for a small addition of krypton. The IEF can only become marginally unstable as the velocity space gap between the the argon and xenon peaks increases. This trend continues until the critical velocity difference equals the difference between the individual Bohm speeds of argon and xenon ions, in which case the IEF is effectively turned off, at least in the plasma. This trend is noticeable in the solid theory curves and in the measured argon and xenon ion sheath edge flow speeds. However, the measured speeds and the model predictions do not everywhere agree within experimental error, as the theory prediction is faster (slower) for the argon (xenon) ions, up until the instability turns off. And the experimental data indicate that the IEF turns off at a relative krypton ion density of roughly 60%–65% while the theory curves indicate a higher relative density, roughly 85%. The uncertainties on the data points included a conservative or maximum estimation of error on the sheath-edge and $v = 0$ determination. These uncertainties were systematic, as the method of sheath-edge and $v = 0$ determination is consistent for all measured velocities of any given ion species. The scattering of the data points is not random, leading to visible trends of the data. The overall agreement is qualitative.

Figure 6 shows results in the case for which neon is added as the third ion, with the argon and xenon ion sheath edge drift velocities graphed as data points, the flow speeds for the onset of the instability and flow locking graphed as solid curves, and the individual Bohm speeds as dashed lines. Here, we observe different trends than the krypton case in which an ion of intermediate mass was added. The theory curves now indicate that until a relative concentration of neon exceeds 90%, the critical $\Delta v_{23}$ between argon and xenon ions does not begin to increase as was expected heuristically. Further the instablility does not turn off until the relative concentration is well above 90%, also as expected. These trends are indeed apparent in the measured sheath edge flow speeds, although, as with the case of krypton, the measured sheath edge flow speeds reach their individual Bohm speeds at a relative neon ion density closer to 80%, somewhat smaller than indicated by the theoretical model. Again, the agreement is qualitative. The phenomena is more complex for the argon ion sheath edge flow speed. The argon ion flow speed is seen to reach its own Bohm speed for both low and high relative concentrations of neon ions, not simply because the IEF has been turned off, but also because the IEF has driven the argon ions to that speed.

The individual Bohm speed is still used as the default assumption in the literature for modeling ion flow to the plasma boundary in multiple ion species plasma in a wide variety of bounded plasma systems ranging from processing plasma to the scrape off layer in tokamaks [6, 31]. The chief result of the work presented here is that in a three ion species plasma, this is generally not true. The ion speed at the sheath edge is generally intermediate between the ion sound speed of the system and the individual Bohm speed, where conditions are such that the IEF becomes marginally unstable in the presheath. This was first noted [24] for the case of an intermediate mass ion added to a two ion species plasma unstable to the IEF, and is now confirmed for the case in which the added ion is less massive than the other two, and which is found to be understandable using the same theoretical framework.

## Acknowledgments

This work was partially funded by the US Department of Energy (DOE), through grant DE-SC00114226, and by the National Science Foundation through grants 1464741, 1464838. The work of SDB was supported by US Department of Energy Grant No. DE-SC0016473.

## References

[1] Tonks L and Langmuir I 1929 *Phys. Rev.* **34** 876
[2] Riemann K-U 1991 *J. Phys. D: Appl. Phys.* **24** 493
[3] Bohm D 1949 *Characteristics of Electrical Discharges in Magnetic Fields* ed A Guthrie and R K Wakerling (New York: McGraw-Hill) ch 3
[4] Robertson S 2013 *Plasma Phys. Control. Fusion* **55** 093001
[5] Hershkowitz N 1989 *Plasma Diagnostics* ed O Auciello and D L Flamm (Boston, MA: Academic) ch 3
[6] Lieberman M A and Lichtenberg A J 2005 *Principles of Plasma Discharges and Materials Processing* 2nd edn (Hoboken, NJ: Wiley) p 182
[7] Stangeby P C 1984 *Phys. Fluids* **27** 682
[8] Cohen R H and Ryutov D D 2004 *Contrib. Plasma Phys.* **44** 111
[9] Lee D, Hershkowitz N and Severn G D 2007 *Appl. Phys. Lett.* **91** 041505
[10] Severn G D, Wang X, Ko E and Hershkowitz N 2003 *Phys. Rev. Lett.* **90** 145001
[11] Wang X, Ko E and Hershkowitz N 2005 *IEEE Trans. Plasma Science* **33** 631
[12] Baalrud S D, Hegna C C and Callen J D 2009 *Phys. Rev. Lett.* **103** 205002
[13] Baalrud S D and Hegna C C 2011 *Phys. Plasmas* **18** 023505
[14] Yip C S, Hershkowitz N and Severn G D 2009 *Phys. Rev. Lett.* **104** 225003
[15] Hershkowitz N, Yip C S and Severn G D 2011 *Phys. Plasmas* **18** 057102
[16] Severn G D, Yip C S and Hershkowitz N 2013 *J. Instrum.* **8:11** C11020–11020
[17] Baalrud S D, Lafleur T, Fox W and Germaschewski K 2015 *Plasma Sources Sci. Technol.* **24** 015034
[18] Brinkmann R P 2011 *J. Phys. D: Appl. Phys.* **44** 042002
[19] Godyak V A 1982 *Phys. Lett.* A **89** 80
[20] Valentini H-B 1996 *Phys. Plasmas* **3** 1459
[21] Franklin R N 2003 *J. Phys. D: Appl. Phys.* **36** 2821
[22] Valentini H-B and Kaiser D 2015 *Phys. Plasmas* **22** 053512
[23] Chen X P 1997 *Phys. Plasmas* **5** 804
[24] Yip C S, Hershkowitz N, Severn G D and Baalrud S D 2016 *Phys. Plasmas* **23** 050703
[25] MacKenzie K R, Taylor R J, Cohn D, Ault E and Ikezi H 1971 *Appl. Phys. Lett.* **18** 529
[26] Yip C S, Sheehan J P, Hershkowitz N and 2013 *Plasma Sources Sci. Technol.* **22** 065002
[27] Oksuz L, Lee D and Hershkowitz N 2008 *Plasma Sources Sci. Technol.* **17** 015012
[28] Kim N, Huh S, Roh H, Park S and Kim G 2015 *J. Phys. D: Appl. Phys.* **48** 225201
[29] Hershkowitz N, Yip C S and Severn G D 2011 *Phys. Plasmas* **18** 057102
[30] Meige A, Sutherland O, Smith H B and Boswell R W 2007 *Phys. Plasmas* **14** 032104
[31] Brunner D *et al* 2013 *Plasma Phys. Control. Fusion* **55** 095010